INTERNATIONAL ATOMIC ENERGY AGENCY
UNITED NATIONS EDUCATIONAL, SCIENTIFIC AND CULTURAL ORGANIZATION

INTERNATIONAL CENTRE FOR THEORETICAL PHYSICS
34100 TRIESTE (ITALY) · P.O.B. 586 · MIRAMARE · STRADA COSTIERA 11 · TELEPHONE: 2240-1
CABLE: CENTRATOM · TELEX 460392-1

H4.SMR/381-7

# COLLEGE ON ATOMIC AND MOLECULAR PHYSICS: PHOTON ASSISTED COLLISIONS IN ATOMS AND MOLECULES

(30 January - 24 February 1989)

# THEORY AND EXPERIMENT OF ELECTRON COLLISIONS IN LASER FIELDS

W.R. NEWELL

University College London
Dept. of Physics & Astronomy
London, U.K.

INTERNATIONAL CENTRE FOR THEORETICAL PHYSICS

Winter College on Atomic and Molecular Physics:

Photon Assisted Collisions in Atoms and Molecules

Lecture Notes and Background Material for

# THEORY AND EXPERIMENT OF ELECTRON COLLISIONS IN LASER FIELDS

W. R. Newell

## PREFACE

These notes are intended to supplement the lectures and provide some degree of background material. The material is these 'notes' will be discussed in the lectures and will provide the basis for further extension of the topics.

Three sections have been included in the present notes

SECTION 1.

This is an introduction to experiments which demonstrate the transfer of photons to and from electrons.

SECTION 2.

This is a descriptive introduction to the theory and scattering processes.

SECTION 3.

This gives a basic account of the first attempt to measure simultaneous electron-photon excitation. The experiemntal work will be extended in the lectures.

SECTION 1

Introduction

Some recent experiments which involve the transfer of photons to and from electrons. We will briefly discuss three experiments

(1) Laser and 'free' electron with multiphoton transfer

(2) Laser and 'scattering' electron with single photon transfer

(3) Laser and 'scattering' electron with multi photon transfer

(1) Multiphoton Absorbtion by 'Free' Electrons.

The experiment of Lampré et al. (1979) gives a clear and simple demonstration of 'free' electrons absorbing quanta of radiation from a laser field. The experimental arrangement is shown in Figure ( 1 ).

Details

Laser is a mode locked yttrium-aluminium-garnet (YAG) oscillator. A single pulse is amplified in a 3 stage Nd-glass amplifier. The final pulse is 30ps with unfocussed intensity of $10^{10}$W/cm$^2$.

$\lambda$ = 10643.5Å (1.17eV)

Polarisation is linear.

The laser enters the vacuum ($10^{-8}$ torr) system containing a indirectly heated oxide filament through W1 and leaves via window W2.

The cathode is heated to 800°K and emits electrons with thermal energy $E_t \sim$ 10meV. The electron density is $\sim 10^{10}$/cm$^3$.

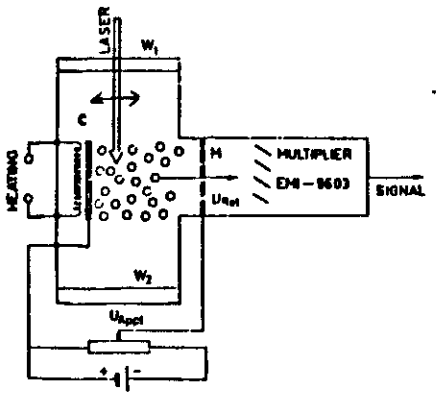


FIG. 1. Schematic diagram of the experimental arrangement. The heated oxide cathode C emits thermal electrons. M is a tungsten mesh biased at the variable negative retarding potential $U_{ret} = U_{appl} - 4.5$ V. The unfocused laser beam enters the glass vacuum vessel through glass window W1. The thin arrow along the axis of the detector shows the direction of the laser electric field as well as the polarization direction.



The electron energy analysis is accomplished using the tungsten grid (M) in a retarding mode. When the grid is -ve w.r.t. the cathode (say a one volt) then none of the initial thermal electrons will pass through the mesh to the multiplier and be detected. However when the laser pulse is present some of these electrons will absorb quanta of radiation.

$n h\nu$ where $n$ = 1, 2, 3 ..... $h\nu$ = 1.17eV

and these electrons $E_t + n(h\nu)$ will then overcome the negative retarding potential and reach the detector (electron multiplier).

N.B. The polarisation of laser is $\perp$ to the cathode surface

$\therefore$ the direction of momentum transfer is 11 to the detector axis - see Figure ( 1 ).

In the experiment by Lampré et al there was an inherent contact potential of 4.5 volts between the cathode and grid

$$\therefore U_{retard} = U_{applied} - 4.5V$$

In the experiment the electron signal was measured as a function of laser intensity I for different $U_{retard}$.

Figure ( 2 ) shows results for $U_{retard}$ = - 4.5V

i.e. $n = \frac{U(retard)}{h\nu} = \frac{4.5}{1.11}$

$= 4$

The electron signal N is $\alpha I^n$

$\ln(N) \alpha n \ln(I)$

This is a general result in multiphoton ionisation.

Similar results were obtained for

n = 3, 5, 6, 7, 8.

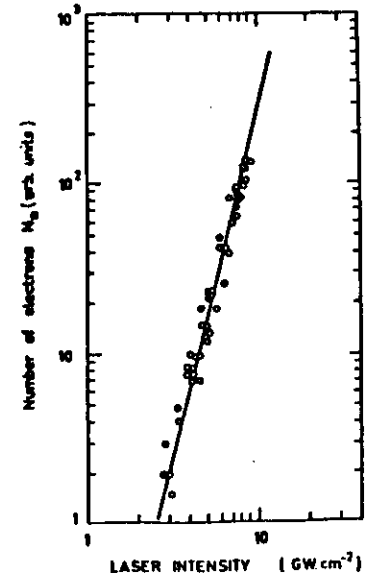


FIG. 2. Log-log plot of the variation of the number of

The cases n = 1 and 2 were not observable as the positive voltages required induced a high background current in the multiplier.

Consider possible mechanism for the process of photon absorption.

(i) Gradient force in the focussed laser.

(ii) Photon absorption by free electrons.

Not possible to conserve energy and momentum simultaneously in a 2-body collision.

(iii) Photon absorption by free electron in presence of THIRD body.

In this case the third body is an 'effective potential' produced by the cloud of electrons.

The photon absorption process can be described by the equation (atomic units)

$$\left(\frac{d\sigma}{d\Omega}\right)^n = \frac{P_f}{P_i}\left(\frac{d\sigma}{d\Omega}\right)^{\text{elastic}} J_n^2\left(\frac{E \cdot Q}{\omega^2}\right)$$

where $\omega$ is photon frequency

$E$ is amplitude of electric field

$Q$ is the momentum transfer $= \underline{P}_f - \underline{P}_i$

$\left(\frac{d\sigma}{d\Omega}\right)^{\text{elastic}}$ is the elastic cross section in the 'effective potential'.

Since $\varepsilon_i \sim 10$ meV

$\varepsilon_f \sim 1.17$ eV then $|P_f| \gg |P_i|$

$Q = P_f - P_i = 0.2933 - 0.08570$ $\qquad P = \left(\frac{\varepsilon}{13.6}\right)^{1/2}$

$n = 3 \quad Q = P_f - P_i = .50702 - .08575$

$\simeq .42227$ a.u.

$\lambda = 10643\text{Å} \Rightarrow \omega^2 = 7.9445\ 10^{23}\ 4\pi^2$

$= 7.9446\ 10^{23}\ 4\pi^2/(4.13\ 10^{16})^2$ a.u.



$E = \frac{2.74\ 10^6}{5.14\ 10^9}$ V/cm a.u.

$\therefore \frac{E \cdot Q}{\omega^2} = 0.23$

n = 3 argument of Bessel function is 0.23

n = 8 " " " " " 0.37

i.e. slow change $\therefore$ can write $J_n^2(\chi) \simeq (\frac{1}{2}\chi)^{2n}(n!)^{-2}$

$\therefore \quad \left(\frac{d\sigma}{d\Omega}\right)^n \propto \left(\frac{E \cdot Q}{\omega^2}\right)^{2n}$

$\propto (E^2)^n$

$\propto I^n$

This relation was observed experimentally - see Figure (2).

What is the nature of the effective potential?

(i) a collective free electron oscillation

(ii) space charge repulsion

(iii) is there any electron coupling with the surface of the cathode?

(iv) influence of background gas as third body

(2) Scattering electron with single photon transfer.

The first experiment which demonstrated the absorption and emission of a single photon in elastic scattering was performed by Andrick and Langhans in 1976 (Ref.2). Similar experiments were reported in 1983 by Curry et al.

The scattering process is

$$e_E + \text{ATOM} + n\hbar\omega \rightarrow e_{E \pm \hbar\omega} + \text{ATOM} + (n \pm 1)\hbar\omega.$$

Since the scattering is ELASTIC the target atom always remains in the ground state.

The laser in all experiments is a $CO_2$ c.w. (polarised).

When the electron 'elastically' scatters it suffers a momentum change $Q(= P_f - P_i)$ and the atom will recoil. During this process in the presence of the laser field the electron can

(1) Absorb a photon from radiation field $n\hbar\omega \rightarrow (n-1)\hbar\omega$
and increase its energy to $E + \hbar\omega$

INVERSE BREMSSTRAHLUNG.

(2) Emit a photon to radiation field $n\hbar\omega \rightarrow (n+1)\hbar\omega$
and reduce its energy to $E - \hbar\omega$

STIMULATED BREMSSTRAHLUNG.

Consider the experiment of Andrick and Langhans - see Figure (3)

$CO_2$ 50 Watt laser $\hbar\omega = 1.17$ meV 90% polarised

Target is argon gas

E = 5, 11.15, 16 eV

electron energy spread is $\Delta E = 40$ meV

Note the important requirement $\Delta E < \hbar\omega$.

Scattering was observed at $\theta = 160^0$ to maximise signal as it is proportional to $Q^2$.

Laser beam was scanned through electron and gas beams.

Problem with electron beam tail -



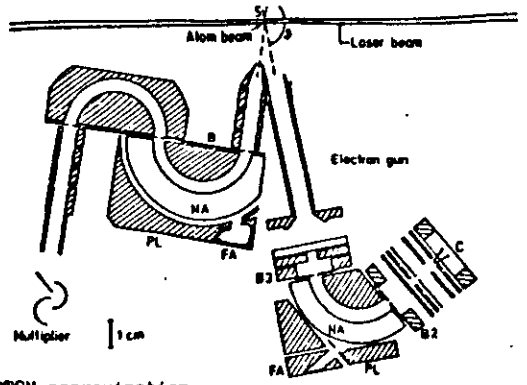


Fig 3.

In the SOFT PHOTON approximation

$$\left(\frac{d\sigma}{d\Omega}\right)^{n=1} = \frac{P_f}{P_i}\left(\frac{d\sigma}{d\Omega}\right)^{el} J_1^2\left(\frac{E\cdot Q}{\omega^2}\right)$$

becomes

$$= \Gamma^2\left(\frac{d\sigma}{d\Omega}\right)^{el} \qquad \left[\Gamma^2 \sim 10^{-3}.\right]$$

$$\Gamma^2 = 4.86\ 10^{-13}\ \lambda^4\ E\ I\ \sin^2\frac{\theta}{2}\ \cos^2\alpha.$$

$$\gamma^2 = \Gamma^2/I$$

where $\lambda$ is wavelength in μm

E is electron energy in eV

I is laser interacting in Watts/cm$^2$

Q is electron scattering angle $\theta = 160^0$

$\alpha$ is angle between Q and laser polarisation.

Results

The energy loss spectrum allowed is given in Figure (4).

The difference between laser 'on' and 'off' signal is X2000.

Since the "interaction volumes" are not equal the laser was scanned to simulate a spatially constant laser power density.

Comparison of $\gamma^2$ calculated from equation A with the measured values is given in Figure (5).

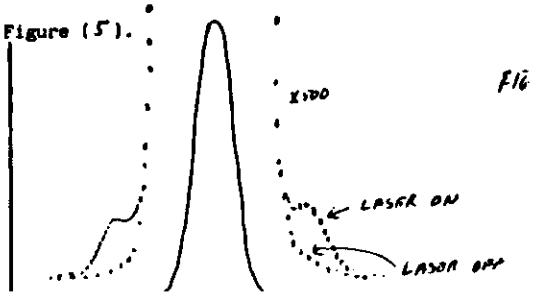


Fig (4)

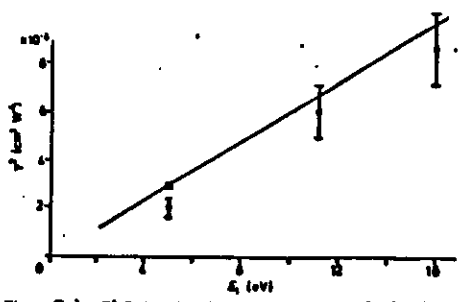

Figure $\gamma^2 = \Gamma^2/F$ plotted against the electron energy $E_1$. Full line: soft-photon approximation; ■: Geltman (1973); ●: this work.

In general agreement is good. The data print of Geltman was computed using elastic scattering wavefunctions calculated using a model potential.

Extension to shorter wavelength.

Bader has repeated this work using a CO laser for $\theta = 160^0$, $E = 11.06$ eV.

Laser. $\lambda = 5.3$ m $\hbar\omega = 234$ meV polarisation 93%

20 Watts c.w. focussed to 1.5 mm diameter.

$$\gamma^2 = 3.93\ 10^{-3} \pm 16\%$$

Soft Photon approx. gives expected value of $4.11\ 10^{-3}$.

Effect of intermediate states.

Essentially these free-free processes are transitions between continuum states of electron + atom. The presence of negative ion states ($\tau \sim 10^{-14}$ s) could enhance the measured cross-section by increasing the strength of the electron-atom coupling.

(3) Electron scattering with multiphoton transfer.

The first experiment to observe multi-photon transfer in free-free scattering was performed by Weingartshofer et al. in 1977 (Ref.6).

Essentially the experiment is the same as Andrick and Langhans but now the laser is pulsed.

$\lambda = 10.6$ μm laser is multimode!

$I = 10^9$ W/cm² an increase of ~$10^6$!

$\therefore \Gamma^2 \sim 50$ and not ~$10^{-4}$ $\therefore$ Perturbation expansion w.r.t. the laser



The laser has a pulse of 2μs.

Spectrometer resolution $\Delta E = 55$ meV

$E = 11$ eV.

Laser polaration // to Q and variable.

Note the multi-photon transfers up to $n = \pm 3$.

With the higher laser intensity the $n = 1$ peak is $5 10^{-2}$ of the primary elastic peak whereas in Andrick and Langhans' expt. it was $5\ 10^{-4}$

Note also the significant redistribution of electron flux.

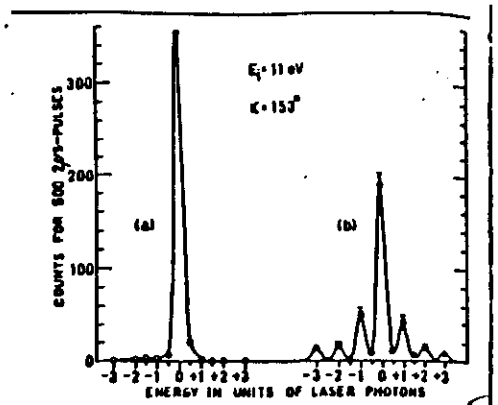


FIG. 6 Energy-loss spectrum of $e^-$-Ar scattering. (a) Without laser field. The circles show the measured experimental points and the estimated outline of the process is drawn with a solid line, which was obtained by tracing out the elastic peak with a ratemeter and scaled to fit the maximum counts. (b) With laser field. The circles with error bars show the measured points and the estimated outline of the multiphoton (emission and absorption) processes are drawn in with solid lines obtained by scaling down the elastic peak as in (a).

In fact flux is conserved and the area under the features is equal in both spectra. This is in fact a sum rule.

The problem with a pulsed source of radiation is the pulse has a temporal distribution of intensity $\sigma^{FF}$(at 1) + $\sigma^{FF}$(at 2)

In order to allow for this varying intensity Weingartshofer (1979) correlated the free-free signal with time windows in the pulse.

In addition the observed free-free signal is dependent on

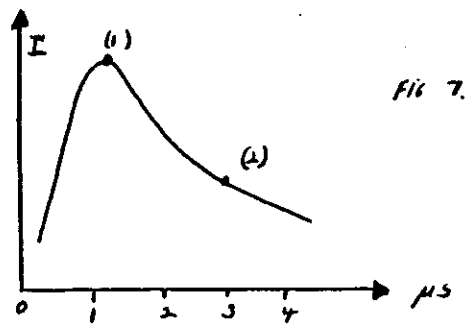


Fig 7.

1) $\theta$ scattering angle (See Figure 8) which compares $\theta = 20^\circ$ and $144^\circ$.

The larger scattering angle produces a greater Q and ∴ a bigger $(\frac{d\sigma}{d\Omega})^{FF}$.

2) By changing , the direction of the laser polaratiom in the scattering plane also changes the $(\frac{d\sigma}{d\Omega})^{FF}$.

3) When

$$\epsilon \cdot \vec{Q} \neq 0$$

no signal is seen.

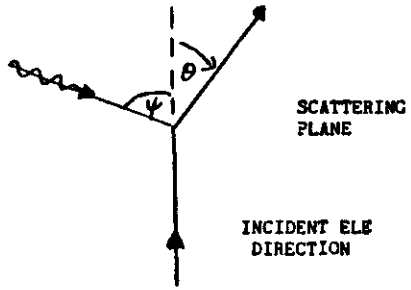


4) When $\epsilon$ is $\perp$ to scattering plane almost no signal is seen.

Perhaps their laser is not 100% polarised.

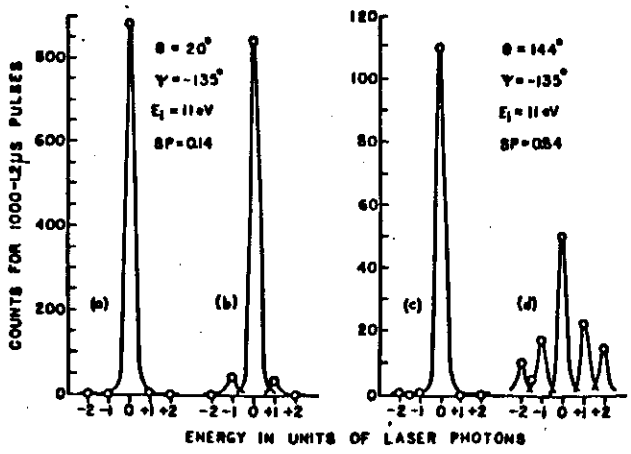


FIG. 8 Energy gain-loss spectra for e-Ar scattering showing dependence on electron scattering angle $\theta$. (a) and (c) without laser, (b) and (d) with laser. $SP = \vec{\epsilon} \cdot (\vec{p}_f - \vec{p}_i)/2p_i$. O measuring points and for solid line see Fig. 3




Summary

The main features of photon absorption and emission by electrons in a potential are demonstrated. The interdependence of Q and $\epsilon$ is clearly demonstrated and also the power dependence.

The nature of the potential has been shown to be either

(a) elastic scattering potential

or (b) effective interaction of electron cloud.

In elastic free-free this work is extendable to a study of

(a) Polarisation Potentials; $e + Na + m\hbar\omega$

(b) Permanent Dipole potentials; $e + HCl + m\hbar\omega$

(c) Resonance interactions.

(d) Inelastic scattering processes.

(e) Open shell systems.


Resonances in the free-free cross-section.

The experiments which have so far looked at resonances in the free-free scattering channel are by Langhans 1978, Andrick and Bader (1984) and Bader (1985).

The results by Langhans (using the apparatus of Andrick & Langhans) for resonance excitation in the free-free n = -1 channel in argon are given in Figure (9).

The core split resonances, ($^2P_{1/2}$, $^2P_{3/2}$) in Argon occur at 11.170 eV and 11.098 eV.

Since the lower spectrum is of the n = -1 channel the analyser is set to detect electrons of energy $E - \hbar\omega$; where E is the incident electron energy.

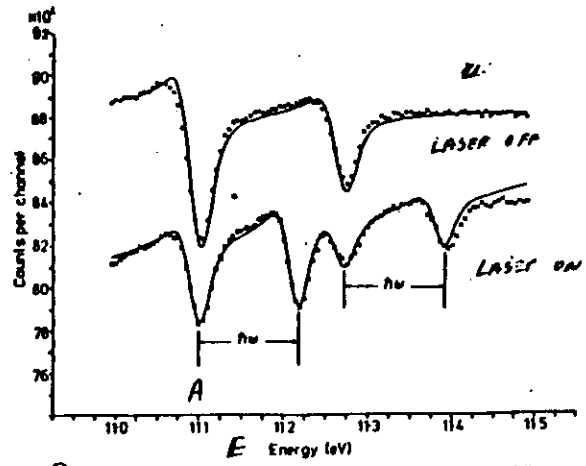


Figure 9 Upper curve: differential elastic cross section for $e^-$-Ar, $\theta = 160°$; full curve: calculated; open circles: measured. Lower curve: differential free-free cross section for $e^-$-Ar, $\theta = 160°$; full curve: calculated; crosses: measured.

Each resonance feature in the elastic channel will produce 2 features in free-free channel.

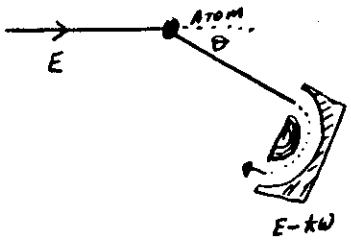


When $E = E_f$ the scattered electrons are only detected if they emit a photon <u>after</u> the resonance scattering. This produces feature A.

When $E = E_f + \hbar\omega$ the incident electron emits a photon <u>before</u> the scattering and comes into resonance and the scattered electron is detected by analyser which is sitting at $E_f$. Similar for $n = +1$ free-free channel.

Spectrum took 100 hours to collect data.

<u>Note some points.</u>

(1) good agreement (full curve) with soft photon approximation.

(2) resonance shape in free channel is very similar to resonance in elastic channel.

(3) no information in the experiment on polarisation dependence ($\varepsilon$ ^ Q).

This work has been extended to the 19.3 eV helium resonance at scattering angles of $20^\circ$, $70^\circ$ and $160^\circ$ (Andrick & Bader 1984). Detection is in the $N = +1$ free-free channel. Work in neon has been reported by Bader.

# SECTION 2

<u>Introduction</u>

The interaction of intense e.m. radiation with atoms and molecules, or more specifically with the electrons bound in these atoms and molecules, leads to new processes which cannot be explained in terms used in the physics of weak e.m. field interactions. These new "multi-photon" processes require intense e.m. for their observation. This is not surprising since the spontaneous TWO-PHOTON decay of atomic hydrogen $H(2S) \rightarrow H(1S)$ is a very weak process; therefore the observation of the reverse process of TWO-PHOTON excitation will require intense photon beams if it is to be readily detected (note however the two-photon decay of H(2S) is the most probable decay for the metastable state).

Typical of the intensities are $10^6 w/cm^2$ to $10^{17} w/cm^2$. With focussed fluxes of $10^{25}$ photon/cm$^2$ to $10^{36}$ photon/cm$^2$. Laser pulse($\tau$) durations are normally in the range $10^{-8}$ to $10^{-12}$ sec. With C.W. lasers intensities are normally a few Watts to $10^5$ w/cm$^2$ (focussed) and dependent on wavelength with the $CO_2$ laser (10.6 $\mu$m) capable of kilowatt outputs(unfocussed).

For example, with a pulsed laser $\tau = 5\ 10^{-9}$s

$I = 10^{16} w/cm^2 \equiv 5\ 10^{28}$ photon/cm$^2$/sec.

Now use this to measure a SINGLE photoionisation cross section $\sigma = 10^{-18}$ cm$^2$.

Then the probability (P) of single-photon ionisation is $P = \sigma I \tau$ (during the laser pulse $\tau$ ) $= 25 >> 1$

i.e. <u>all</u> atoms in the interaction region, during $\tau$, will be ionised. Even in an intense synchrotron source the photon flux is only $\sim 10^{14}$. Therefore P would be $= 10^{-26}\ 10^{14}\ 10^{-5} = 10^{-11}$ with the synchrotron pulse duration of $10^{-5}$ secs.

Let us consider TWO-PHOTON EXCITATION/IONISATION (See Figure (a)

Assume $2\hbar\omega > $ I.P. We could also use the same arguments for simultaneous electron-photon ionisation via a discrete (stationary state) $E_1$, which has a lifetime $\tau_1$.

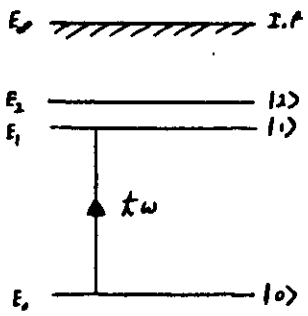


$\sigma_0$ = absorption cross-section going from $|0\rangle$ to $|1\rangle$

$\sigma_1$ = ionisation cross-section

Then the total Transition Probability/time for absorption followed by ionisation is

$$T_2 = (\sigma_1 I)\,\tau_1\,(\sigma_0 I) = (\sigma_1\tau_1\sigma_0)\,I^2 = \sigma_2 I^2$$

where $I$ is the photon flux and 2 denotes the order of the reaction

with $\sigma_0 = 10^{-16}\,cm^2$, $\sigma_1 = 10^{-19}\,cm^2$ $\tau_1 = 10^{-3}$ sec

then $\sigma_2 = 10^{-61}\,cm^4$ sec. However the small value of $\sigma_2$ is offset by the large photon flux say $I = 10^{25}$. Then with a pulse duration of $\tau_L = 5\ 10^{-9}$ sec the probability of RESONANT TWO-PHOTON IONISATION during the pulse is

$$\tau_2\,T_2 = 5\ 10^{-2}$$

i.e. 5% of atoms in interaction region are ionised!

Note that with a synchrotron source with $10^{14}$ flux

$$\tau_5\,T_2 = 10^{-5}\ 10^{-61}\ 10^{23} = 10^{-28}$$

$\tau_5$ is the synchrotron pulse duration.



NON-RESONANT TWO-PHOTON (PHOTON-ELECTRON) EXCITATION.

Now $\hbar\omega \neq (E_1 - E_0)$

But $2\hbar\omega > $ I.P.

Let us consider a qualitative picture. In this case the photon 'excites' a virtual state $|i\rangle$ i.e. not a real atomic state. This virtual state is in general described as a linear superposition of all the real atomic states $|n\rangle$ which are connected to $|0\rangle$ by an electric dipole transition.

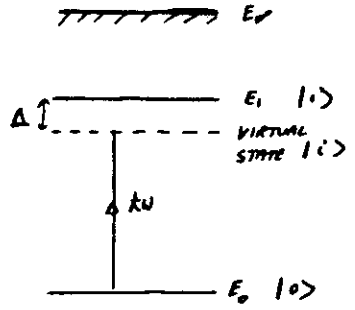


Therefore can write $|i\rangle = \sum_n \alpha_n |n\rangle$.

The coefficient $\alpha_n$ can be determined (Lambropoulos 1976).

The virtual state $|i\rangle$ will have a lifetime $\tau_i$ given by the inverse of the magnitude of the detuning $\Delta$ from the nearest real state $|n\rangle$. This argument is not exact but we will use $\tau_i = \Delta^{-1}$ as a working rule to give us a feel for the excitation process. In this case $\hbar\omega + \Delta = E_1 - E_0$ (see Figure b ). Now we have for the non-resonant transition probability/time

$$T_2 \sim \sigma_i\, I\, \frac{1}{\Delta}\sigma_0\, I = \sigma_2 I^2$$

$\sigma_0 = 10^{-16}\,cm^2$ for photon excitation

$\sigma_i = 10^{-19}\,cm$ for electron ionisation

$\tau_i = 10^{-15}$ sec.

Then $\sigma_2 = 10^{-50}\,cm\ sec^4$ which is $\underline{10^7}$ smaller than $\sigma_2$ for resonance two-photon (photon-electron) ionisation.

Consequently any experiment which relies on virtual states as the intermediate stages will be much reduced in detectable signal. It should also be noted that the concept of "cross section" loses its classical meaning in the case of virtual

GENERALISATION OF N = 2 CASE.

The above discussion has been concerned with a 2-stage or a second-order process (N = 2 i.e. $T_N$ ). This can be generalised.

We have defined $|i\rangle = \sum_n a_n|n\rangle$ and the ionisation of $|i\rangle$ can be determined using the bound-free matrix element

$$\langle f(k)\,|\, e\,\underline{\epsilon}\cdot\underline{r}\,|i\rangle$$

where $e\,\underline{\epsilon}\cdot\underline{r}$ is electric dipole operator

$\underline{\epsilon}$ is *polarisation* direction of laser field

$f(k)$ is the continuum state. $k = \frac{1}{\hbar} k^2/m$.

The coefficient $a_n$ can be determined in terms of

(i) The detuning $\Delta \equiv \hbar\omega - (E_n - E_o)$

are (ii) The strength of the dipole transition $\langle n|\underline{\epsilon}\cdot\underline{r}|o\rangle$

as $a_n = \frac{\langle n|\epsilon\cdot r|o\rangle}{(E_o - E_n - \hbar\omega)}$ .

Consequently $\sigma_{N=2} = (\text{constant})\; k\,\omega^3 \int |M^2_{fo}|^2 d\Omega_k$

where $k$ is the direction of the outgoing photo electron and the second-order (N=2) matrix element is

$$M^2_{of} = \sum_m \frac{\langle f|\epsilon\cdot r|m\rangle\langle m|\epsilon\cdot r|o\rangle}{(E_m - E_o) - \hbar\omega} ,$$

Therefore the second-order excitation requires an infinite sum over the intermediate states both discrete and continuum.

In the case of N = 3 transition

$$M^3_{fo} = \sum_n \sum_m \frac{\langle f|\epsilon\cdot r|n\rangle\langle n|\epsilon\cdot r|m\rangle\langle m|\epsilon\cdot r|o\rangle}{(E_n - E_o - 2\hbar\omega)(E_m - E_o - \hbar\omega)}$$

The extension to the general case is obvious.

$$\sigma_N = (\text{constant})\; k\,\omega^N \int |M^N_{fo}|^2 d\Omega_k$$

and the Transition Probability/time is

$$T_N = \sigma_N I^N$$

$$\sigma(\text{cm}^{2N}\,\text{sec}^{N-1})$$



Radiation Effect in SEPE.

It has been suggested by Lambropoulos that the energy loss peak associated with SEPE may be masked by radiation line broadening. Consider in particular SEPE in hydrogen with electron $E_i$ and Nd laser $\hbar\omega$ = 1.17 eV.

When $E_i > E_1$ (see Figure c) then the energy loss spectrum of the electron will consist of three types of peaks (see Figure d)

(i) elastic $E_i$

(ii) direct excitation of 2S level at $(E_i - E_1)$

(iii) SEPE of 2S level at $E_i - E_1 \pm \hbar\omega$.

This particular process has not yet been detected but it has been discussed in calculations by Jetzke et al. 1984.

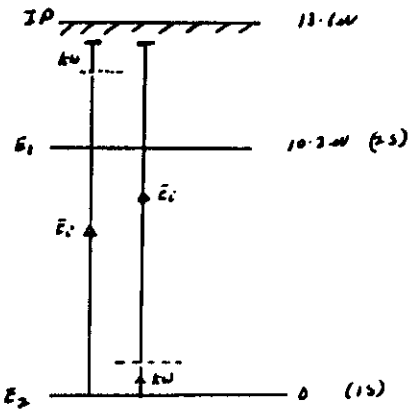


Fig (c) HYDROGEN

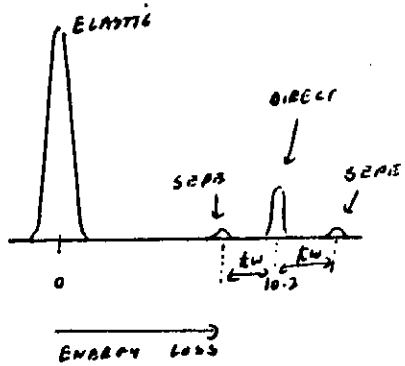


Figure d

The question arises as to the influence of the laser beam $10^{13}$ w/cm$^2$ on the n = 2 levels.

Since $E_{IP} - E_1$ = 3.4 eV then three-photon ionisation of the level is possible by the laser beam!

Since the final state of the SEPE excitation is a state which can 'decay' (the decay rate in this case is 3 $\hbar\omega$ ionisation) then the 2S level will be broadened. Consequently the energy loss peak $(E_i - E_1 \pm \hbar\omega)$ will also be broadened by the same amount.

The broadening is given by $T_3 = \sigma_3 I^3$

$\sigma_3 = 1.5\ 10^{-78}\ cm^6\ sec^2$

$I = 10^{12}\ w/cm^2 = 0.6\ 10^{31}\ photon/cm^2/sec$

$\hbar\omega = 1.17\ eV.$

Therefore $T_3 \gtrsim 3\ 10^{14}/sec.$

Using $T_3^{-1} \Delta E = \hbar$

$\Delta E = 6.6\ 10^{-34}\ 3\ 10^{14}/1.6\ 10^{-19}$

$\gtrsim 1.2\ eV$

Therefore broadening 1.2 eV > $\hbar\omega$ (1.17 eV). Consequently the SEPE peaks will merge into the direct peak. If higher laser powers are used then there will onl be a base widening of the direct peak detected! However with lower powers $\sim 10^{12}$ w/cm² the broadening will only be 12 meV!

This argument supposes that the SEPE process is sequentially followed by three-photon ionisation. That also is a power-dependent process.

ELECTRON ATOM SCATTERING IN LASER FIELD

The first modern discussion of combined scattering of electrons, atoms and photons was given by Göppert-Meyer in 1931 (in her thesis) using second-order perturbation theory. Symboc i ally the problem can be written as

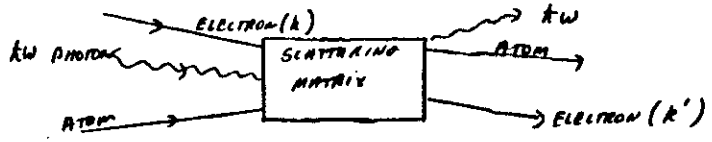


in a universal treatment. However any 'real' theory must make concessions to the parameters involved, i.e.

(1) laser frequency w and polarisation

(2) laser power

(3) electron energy and spin polarisation

(4) nature of the "atomic target"



As well as this there is the consideration as to how the scattering reaction actually proceeds. Is there an instantaneous interaction or a time-evolved scattering scheme and in what sense do the 3 'particles' interact in pairs; electron-photon, photon-atom, electron-atom; is there a hierarchy of the 'pair' interactions and what determines it? Any rigorous solution must be able to account for all these factors, but an exact solution is ideal and we normally proceed by various levels of approximation. Even in the two-body problem of electron-atom scattering the multiplicity of scattering channels and the variation of scattering parameters requires the severe introduction of approximations, e.g. Born, DWPO, R-MATRIX, Impulse, Close Coupling, Variation Techniques for particular scattering processes. If, in addition, we add a radiation term then we can see how quickly the complexity of Scattering Matrix S will grow.

$$\Psi(FINAL) = S\ \Psi(INITIAL).$$

In electron atom scattering we have (a) elastic scattering, (b) excitation and (c) ionisation. These, with the presence of a radiation field can be written as

(A) $e(E_i) + m\hbar\omega + A(E_o) \rightarrow e(E_i \pm \hbar\omega) + A(E_o) + (m \pm 1)\hbar\omega$

(B) $e(E_1) + m\hbar\omega + A(E_o) \rightarrow e(E_1 - E_1 \pm \hbar\omega) + A^+(E_1) + (m \pm 1)\hbar\omega$

(C) $e(E_i) + m\hbar\omega + A(E_o) \rightarrow e(E_i - I\ P\ \pm \hbar\omega) + A^+ + (m \pm 1)\hbar\omega + e(E_e)$

In (A) the atom remains in the ground state $E_o$ and plays the passive role of a third body while the electron absorbs (N = + 1) or emits (N = - 1) a photon (considering only single-photon transfer). This process is stimulated Bremsstrahlun and the electron and radiation fields interact with the 'recoil' provided via the elastic scattering potential. In (B) the incident electron also excites the atom from state $E_0$ to $E_1$ and interacts with the radiation field with a photon transfer. In case (C) the atom is ionised but again with photon transfer to the electron. In this case the ejected electron ($E_e$) does not interact with radiation field. As we go from A to C there is a change in the coupling of the electron to the atom and this will modify the absorbtion/emission of photons.

This is of course the multi-photon extension of these processes where $N > 1$.

In general, the electron-atom-radiation system can be expressedd as (in a perturbation treatment)

$$
\begin{aligned}
H = {} & H_{AT}\ (\text{atomic}) \\
& + H_{e}\ (\text{electron}) \\
& + H_{RAD}\ (\text{radiation field}) \\
& + H_{e\text{-}AT}\ (\text{electron-atomic}) \\
& + H_{AT\text{-}RAD}\ (\text{atomic-radiation field}) \\
& + H_{e\text{-}RAD}\ (\text{electron-radiation field})
\end{aligned}
\qquad
\begin{aligned}
&\Big) \\
&\Big) \\
&\Big) \text{ separate Hamiltonians} \\
&\Big) \\
&\Big) \\
&\Big) \\
&\Big) \text{ interaction Hamiltonians} \\
&\Big)
\end{aligned}
$$

Resonant Interaction

If the laser is resonant with a stationary atomic state (see Figure e ) either by $\hbar\omega_1 = E_0 - E_1$ or by $n\hbar\omega_2 = E_0 - E_1$ then we will have electron scattering from a *pumped* state with the $H_{AT\text{-}RAD}$ term on resonance. Experiments of this single-photon type have been done by Hertel et al. (198 ) in sodium and Trajmar et al. (198 ) in barium. We are not concerned with the processes in which the 'atomic + radiation' state lives for a long period of a few nanoseconds. In addition, the electron can have a quasi resonant excitation if the incident electron energy $E_i$ is resonant with a Feshbach resonance. eg. $E_i$ = 19.3eV helium negative ion resonance. In this case the negative $A^-$ is formed for $\tau = 10^{-14}$s.

Again we are not directly concerned with the processes. In SEPE we will exclude any form of resonant coupling of either electron or photon to the atomic target.

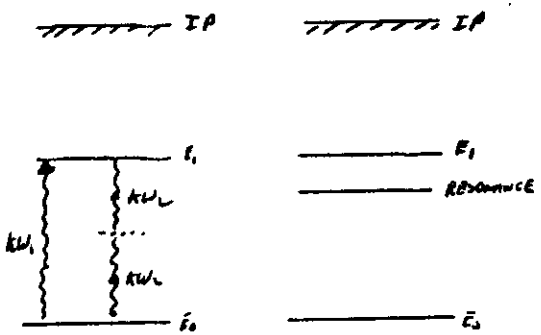


Figure (e)



Non-Resonant Interaction

In this case electron-radiation and atom-radiation terms are equally important but not necessarily of equal strength. Indeed it is known that as $\omega \to 0$ the atom becomes 'transparent' to the laser field and the atom-radiation term can be ignored. In these non-resonant photon cases the atomic structure will be very important.

SEPE

In case (b) it is possible for the transition from $E_0$ to $E_1$ to occur but without the electron losing $(E_1 - E_0)$ if the photon can be used to 'bridge the gap'. We can consider several combinations of $E_i$ and $\hbar\omega$ as in Figure (f).

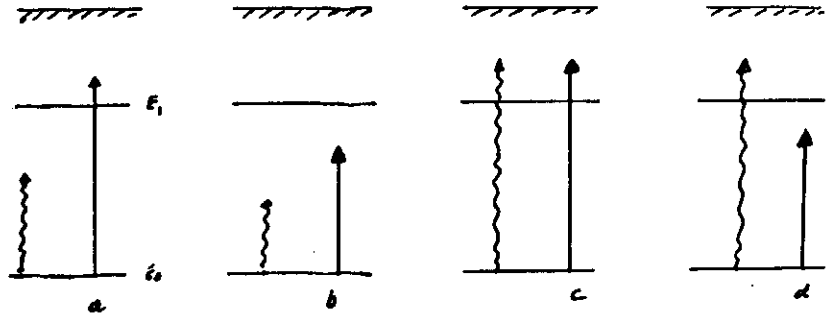


Figure f

In figure f the $\perp$ height of the lines represent the energies of the photon ($\rightsquigarrow$) and electron ($\longrightarrow$). Neither energy is resonant with any level. In cases a and c the electron can separately excite the level $E_1$ and in no case can the photon separately excite $E_1$. In cases c and d the electron is scattered with an increase in its energy which arises from the surplus of photon energy over $E_1$ - i.e. the electron is SUPER ELASTICALLY SCATTERED. In cases a and b the electron will lose energy in exciting $E_1$ with the photon. In case b it requires BOTH the photon and electron to excite the state $E_1$ i.e. SEPE - a new process.

Let us assume that the radiation field is weak and only lower-order photon processes are applicable. Then perturbation is valid for atom-radiation interaction Using Feynman diagrams the electron-radiation interaction can be described by

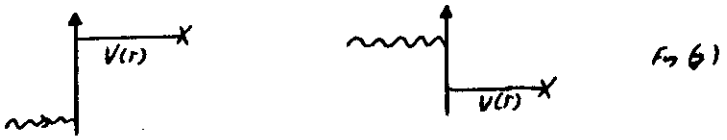


Fig 6)

where V(r) is a local potential replacing $H_{e-AT}$. The photon only couples to the electron. The cross section can be derived from these two amplitudes. This approach will fail when

(a) the radiation intensely increases

(b) the frequency increases

as now the photon also couples to the atom. Consequently we will need 4 diagrams

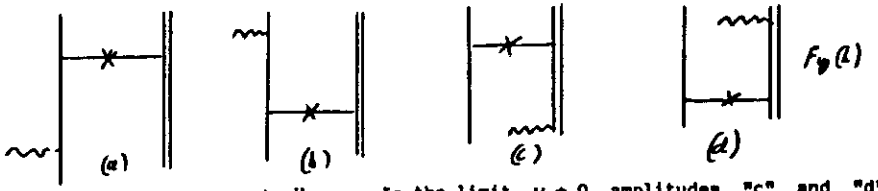


Fig (1)

in which —✕— represent $H_{e-AT}$. In the limit $w \to 0$ amplitudes "c" and "d" go to zero. In a and b the electron is 'dressed' where as in c and d the atom is 'dressed'.

It is not always possible to use perturbation theory especially in the very interesting areas of threshold excitation and when there is any 'resonance' interaction. The simplest way to proceed is normally to require that the $H_{AT-RAD}$ interaction is neglected - i.e. neglect Feynman diagram c and d. Now all the radiation coupling to the scattering process is via the electron and the interaction of the electron and atom is treated with a potential V(r).

The solution of the Schrödinger equation for the interaction of a charged particle and a plane electromagnetic wave can be solved exactly and is called the Volkov solution (see Rosenberg 1939) and can be visualised using Feynman



diagrams as in Figure (1) where ⫲ represents the Volkov solution. It is clearly seen that this consists of an infinite number of amplitudes given in increasing order of photon coupling, i.e. a is zero order, b and c first order, d e f g second order etc. Due to the non-conservation of energy and momentum between electrons and photons all the interactions are VIRTUAL. The interactions only become REAL when there is a third body present which will conserve the energy and momentum. The third body is a potential V(r) which of course will also have different orders of interaction with the electron. If we consider the lowest order (i.e. First Born) then the solution of the photon-assisted collision can be written as

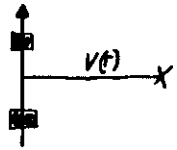


where ⫲ is the dressed electron propagator; virtually dressed to all orders in the radiation field. If in the collision N photons are transferred via the real states formed due to presence of V(r) then the cross section $(\frac{d\sigma}{d\Omega})^N$ can be written as

$$(\frac{d\sigma}{d\Omega})^N = \frac{P_f}{P_i} J_N^2 (\frac{E \cdot Q}{w^2}) (\frac{d\sigma}{d\Omega})^{BORN} \quad \ldots\ldots\ldots \quad (A)$$

where $P_f$ is final electron momentum

$P_i$ is initial electron momentum and Q the momentum transfer.

E is electric field strength and w the frequency

J is a Bessel Function.

Note that this formula is

(i) Correct to all orders in radiation field.

(ii) No restriction has been placed on laser frequency or intensity.

(iii) Providing $(E \cdot Q/w^2) < N$ then Bessel function can be written

$J_N(y) \sim \frac{1}{N!} (\frac{1}{2}y)^N$

which gives the correct low field result, i.e. identical to the lowest order treatment.

(iv) The only restriction is on the order of the scattering which in this case is the 1st Born approximation.

In order to improve on equation (A) we must include the higher-order terms of V(r). Inclusion of the higher-order Born terms can be easily included in schematic form as given in Figure ( ). Mathematical summation of this series would give an exact result but it is difficult. However, by replacing the dress electron propagators (other than the initial and final operabors) by free electron propagators we obtain

$$\left(\frac{d\sigma}{d\Omega}\right)^{N} = \left(\frac{P_f}{P_i}\right) J_N^2 \left(\frac{E+Q}{W^2}\right) \left(\frac{d\sigma}{d\Omega}\right)^{EXACT} \quad \ldots\ldots\ldots \text{(B)}$$

where equation (B) differs from (A) in that now we have the EXACT scattering cross section but one not associated with photon transfer. The physical condition implied in replacing  by  is w is small.

Consequently equation (A) is correct to all orders in photon transfer but only the lowest order in scattering; whereas equation (B) is correct to all orders in scattering but only lowest order in photon transfer.

SECTION 3

## SIMULTANEOUS ELECTRON-PHOTON EXCITATION OF METASTABLE He STATES USING A ND-YAG LASER.

Introduction.

Utilising bosons and fermions to excite discrete atomic states is of fundamental interest to Atomic Physicists as well as having a practical application in high temperature and partially-ionised plasmas encountered in fusion studies. The simultaneous excitation of atomic states (discrete or continuous) when high-density lasers are in use can have cross-sections which exceed the direct electron excitation cross-section.

The object of the experiment is to detect the process $e + h\nu + He \rightarrow e' + He^*$ for incident electron energies near the threshold of the direct reaction $e + He \rightarrow e' + $ and to estimate the cross-section. The experimental arrangement is shown in Fig. . A pulsed electron beam with energy of 19 eV (for example) and a photon beam from a Q-switched Nd-YAG laser intersect in the beam of He atoms from a gas jet. Atoms excited to the 19.8 eV metastable level are detected in a channeltron multiplier 55mm from the interaction region. The laser intensity is of the order of $10^9$ W/cm$^2$. "Laser on" shots at 20pps are interleaved with "Laser off" shots at the same repetition rate in order to subtract background due to the direct excitation of metastables by the high-energy tail of the electron beam. The laser and electron beam firing signals are generated by a CAMAC unit interfaced to a GEC 4080 computer which also logs the time of flight of each event. A schematic diagram of the electronics is shown in Fig. 2.

No experimental, and only a limited amount of theoretical work has been done in this field of research. The scattering process at threshold can be written

$$e(E_i) + h\omega + A(\epsilon_o) = A^*(\epsilon_1) + e(0)$$

where the incident-electron will lose all its energy, $E_i$, in exciting the atomic state ($\epsilon_1$), where $E_i + \hbar\omega = \epsilon_1 - \epsilon_o = \Delta\epsilon$. The general process can be understood

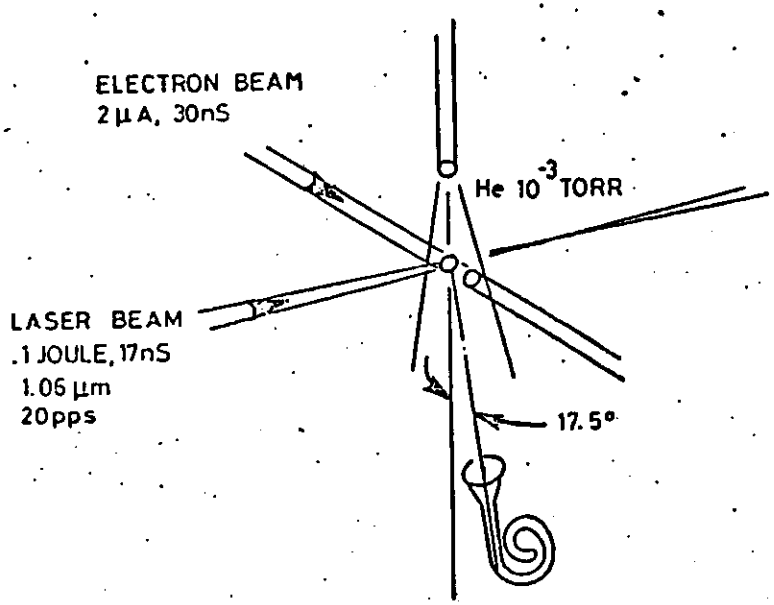


FIG.1. LAYOUT OF EXPERIMENT

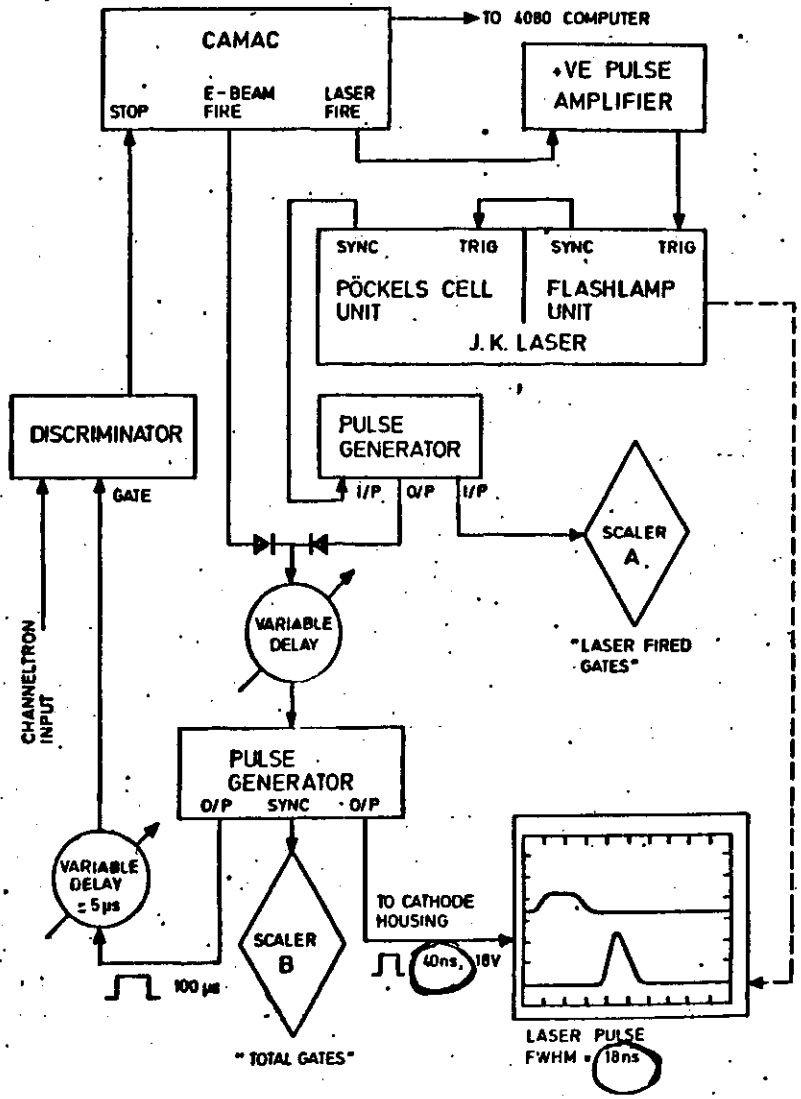


SCHEMATIC DIAGRAM OF ELECTRONICS

FIGURE 2.

by referring to Figure (A) which shows the two discrete atomic states $\epsilon_0$ and $\epsilon_1$ with the incident electron energy $E_i$ and photon energy $\hbar\omega$. Separately neither the electron nor the photon is sufficiently energetic to excite the atom from $\epsilon_0$ to $\epsilon_1$, but the combined energy $E_i + \hbar\omega > \Delta\epsilon$ is sufficient. Excitation of the $\epsilon_1$ state can be detected by observing the energy spectrum of the scattered electron $E_s$ and in this case an energy loss peak at $E_s = E_i - (\Delta\epsilon - \hbar\omega)$ will be observed. If $\hbar\omega > \Delta\epsilon$ then an energy gain peak will occur at $E_s = E_i + (\hbar\omega - \Delta\epsilon)$ analogous to stimulated Raman scattering of light. Note also that if $E_i > \Delta\epsilon$ then the directly excited state will be observed at $E_s = E_i - \Delta\epsilon$. See Figure (B)

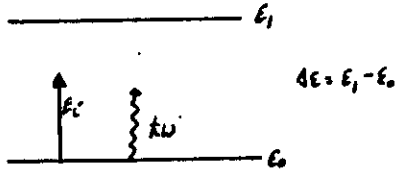


FIG (A)

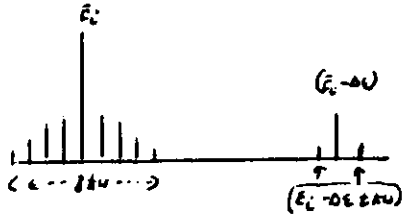


FIG (B)

The electron spectrum will also be complicated by the presence of electrons which have undergone a free-free scattering process in the radiation field resulting in electron features at $E = E_i \pm n\hbar\omega$ where $n$ is the number of photons absorbed or emitted by the electron during the scattering event. In addition, the electron spectra are measured differentially with the need to scan the spectra resulting in lower signal rates and a much increased operational laser time.

In this experiment the cross-section for the electron+photon excitation is measured by detecting the excited atoms directly since the presence of free-free electron features would unnecessarily complicate the analysis of the spectra. Observation of the excited atoms has the dual advantage that since all of the atoms can be detected it is equivalent to making a total electron scattering measurement without the inherent background problems associated with the primary electron beam.



Experimental study of these off the 'energy-shell' collisions is not possible with conventional light sources due to their low intensities, but the high-intensity laser sources now available make these experiments feasible. In particular the already available Nd-YAG laser system at R.A.L. which can produce intensities of $10^{13}$ W/cm$^2$ would permit measurements to be made at intensities where the laser-assisted scattering is of comparable magnitude to the direct scattering. In the first instance the experiment was performed at $\sim 10^{10}$ W/cm$^2$ using an auxilliary laser (JK) of high-repetition rate.

The particular process we intend to study is combining a Nd-YAG laser ($\hbar\omega$=1.17e and a primary electron beam ($E_i$=19eV) to excite the 19.8eV metastable state, $2\,^3S_1$, in helium at 0.37eV above the threshold in the cross-section. A helium target is particularly well suited to this experiment as the two lowest-lying states are metastable at 19.8eV. $2\,^3S_1$. and 20.6eV, $2\,^1S_0$, and helium has the highest threshold against multiphoton ionisation of any gas target. The high internal energy of the metastable state also makes it easy to detect in a surface ionisation detector The advantage of a large photon energy (1.17eV) permits the use of conventional electron gun with a high primary-beam current ($\sim$1μA) and a low-energy resolution of $\Delta E \sim 0.4$eV, which is still sufficient to prevent excitation of the $2\,^1S_0$ state, whereas a $CO_2$ laser ($\hbar\omega$=0.117eV) would require an operational $\Delta E$ of 0.030eV with the resultant reduced primary beam current of $\sim$3 nA. In reality, the 'tail' of the electron beam can produce direct excitation of the $He^*$ hence the experiment will be conducted in a pulsed mode (laser on/off) with the difference signal giving the contribution of simultaneous electron-photon excitation of $He^*$.

The general experimental configuration consists of three mutually-perpendicular beams (atomic, electron and laser) intersecting in a collision region with a common beam overlap of $\lesssim$1mm diameter. The atomic beam is produced with a hypodermic needle located 1mm from the edge of the collision region. The metastable atoms produced drift out from the interaction region and are detected in a channel electron multiplier located 50mm from the interaction region. The detector is suitably oriented to allow for momentum transfer effects to the target due to the scattering

event. The electron beam and the laser beam are both pulsed in order to give maximum discrimination against the background of direct electron excitation events produced by the high-energy tail of the electron beam. The metastable time of flight (~40μs) is recorded and stored in the computer used to control the pulsing system. It gives added discrimination against the detection of scattered electrons and any UV photons which may be produced by multiphoton processes in contaminants. In addition, biasing fields are used to eliminate most charged particles.

The cross-section for the laser-assisted scattering is estimated to be $< 10^{-3}$ of the cross-section for direct scattering, at a laser intensity of about $10^9$ watts/$cm^2$ and thus the feasibility of the experiment depends on the absence of any significant high-energy tail to the electron beam. Since the laser "on" time is only $1.7 \times 10^{-8}$ sec/pulse at a repetition rate of 20pps, a high peak electron beam current is also needed. A normal electron gun is unable to fulfil both conditions simultaneously and the tungsten ribbon filament was replaced with $LaB_6$, a low work function emitter, and suitable conditions were achieved in tests.

Rahman and Faisal (1976) have shown that the simultaneous electron-photon excitation for the H(2S) state of hydrogen is greater than the direct electron impact excitation cross-section providing field intensities of $10^{13}$ W/$cm^2$ are employed. Using the value for the direct electron impact cross-section of the $2\,^3S_1$ helium state we can obtain a working estimate of the expected signal. Hence with $\sigma_{DIRECT}(2\,^3S_1) = 4.4\ 10^{-18}$ $cm^2$ at 0.37eV above the threshold, with $\hbar\omega = 1.17$e I = $10^{13}$ W/$cm^2$, a gas beam pressure of $2 10^{-2}$ torr and a 5μA beam then we can expect a metastable production rate of 60 atoms per pulse. However, allowing for the quantum efficiency of the channel electron detector (50%) and the possible loss of signal due to initial gas beam divergence (50%), this could reduce to 15 counts per laser pulse. Focussing of the laser and electron beams to the required size (1mm dia.) is considerably less of a problem than producing a gas beam of the required dimensions and large signal losses from these beams is not expected. Therefore the experiment is feasible provided the plasma problems associated with high-intensity laser pulses can be overcome.



Although the simultaneous electron-photon process is in general a second-order effect, it only has a first-order dependence on the radiation field. Hence an intensity of $10^{13}$ W/$cm^2$ (= 100 J pulse of $10^{-9}$ s with a spot size of 1mm diameter) is only $\sim 5.10^{20}$ photons and with only 3 pulses per hour (maximum rate available from the Glass Laser at RAL) the total photon flux is $\sim 1.5 \times 10^{21}$ photons per hour whereas a small laser giving 200 mJ pulses but at a repetition rate of 20 pps gives $\sim 7.7 \times 10^{22}$ photons/hour although its intensity is only $\sim 10^9$ watts/$cm^2$. Hence when we study only the first-order process $E_1 = (\Delta\varepsilon_1 - \hbar\omega)$ the signal will increase in proportion to the total photon flux, i.e., 770/15 = 51 and by a further factor of 3 if the pulse energy of the J.K. laser is increased to 600 mJ. Funds will be made available by laser division to upgrade the present J.K. laser to this specification. However, to investigate higher-order effects when 2 or more quanta of radiation are involved in the simultaneous excitation $E_1 = \Delta\varepsilon - n\hbar\omega$, $n > 1$, it is necessary to employ high-density radiation fields in excess of $10^{10}$ watts/$cm^2$, and in this case it will be necessary to use a high-power glass laser facility.

Although the $2\,^3S_1$ metastable is the lowest bound state in helium there exist several Feshbach-type resonances built on $2\,^3S_1$ as a parent state. The lowest of these is $(1s\ 2s^2)^2S$ at 19.3eV with a much weaker resonance at 19.45eV, $(1s2s\ 2p)^2P$, and several in the region 19.5eV to 20.3eV. Such resonance states may assist the simultaneous electron-photon excitation process when $\hbar\omega = 1.17$eV due to the tail of the electron beam exciting a negative ion resonance in the target. In helium the lifetime of the 19.3eV resonance ($\tau$=8.3 $10^{-14}$ s) greatly exceeds the lifetime ($\tau$=5.6 $10^{-16}$ s) of the virtual state produced by the laser field dressing the atom. Hence in order to ensure that only a 'pure' electron-photon excitation is detected it will also be necessary to frequency double the laser to $2\hbar\omega$(=2.34eV) which will remove the possibility of accidental negative ion resonance excitation.

## Experimental Details

### The Electron Beam

A detailed layout of the beam is shown in Fig. 3 with typical voltage settings indicated. The electron source F was originally a tungsten ribbon but changed to a $LaB_6$ crystal. The centre tap of the heater is the reference earth of the system. F is enclosed in a Wehnelt cylinder KH with a 1mm diameter aperture 1mm from the tip of the emitter. The voltage on this cylinder is pulsed - all others are Dc. The voltages on A and L1 are set to focus the emitter on an aperture, 0.7mm in diameter in L1 which is followed by a second aperture of the same diameter to limit the angular spread of the beam. The first aperture is imaged on the interaction region by the gap-lenses between L1 and L3, L3 and L4 The voltage on L4 determines the energy of the beam. The beam is first tuned to give maximum current to the collector L8 and then further optimised to give maximum metastable production when L4 is set to the peak of the excitation curve.

The quality of the beam focus can be judged from vertical scans of the beam across the 3mm diameter aperture in L4, 2.5mm from the gas jet. The sharpness of the cut-off on the aperture measures the beam height, which is only 0.27mm, FWHM. It could well be smaller at the position of the gas jet. The emitting region of the $LaB_6$ source may be as small as 30 μ. This vertical scan is used to centre the electron beam accurately within the aperture.

A horizontal scan gives a convolution of the jet diameter with the beam width. Assuming cylindrical symmetry of the electron beam, we found the jet to be 0.5mm FWHM, which is compatible with the nozzle being 0.4mm in diameter.

The 16 Volt, 30n Sec wide, 7n Sec rise-time pulse applied to KH for both "Laser on" and "Laser off" shots comes from a commercial pulse generator triggered externally. The spread in arrival time of scattered electrons at the channeltron accurately reflects pulse width.

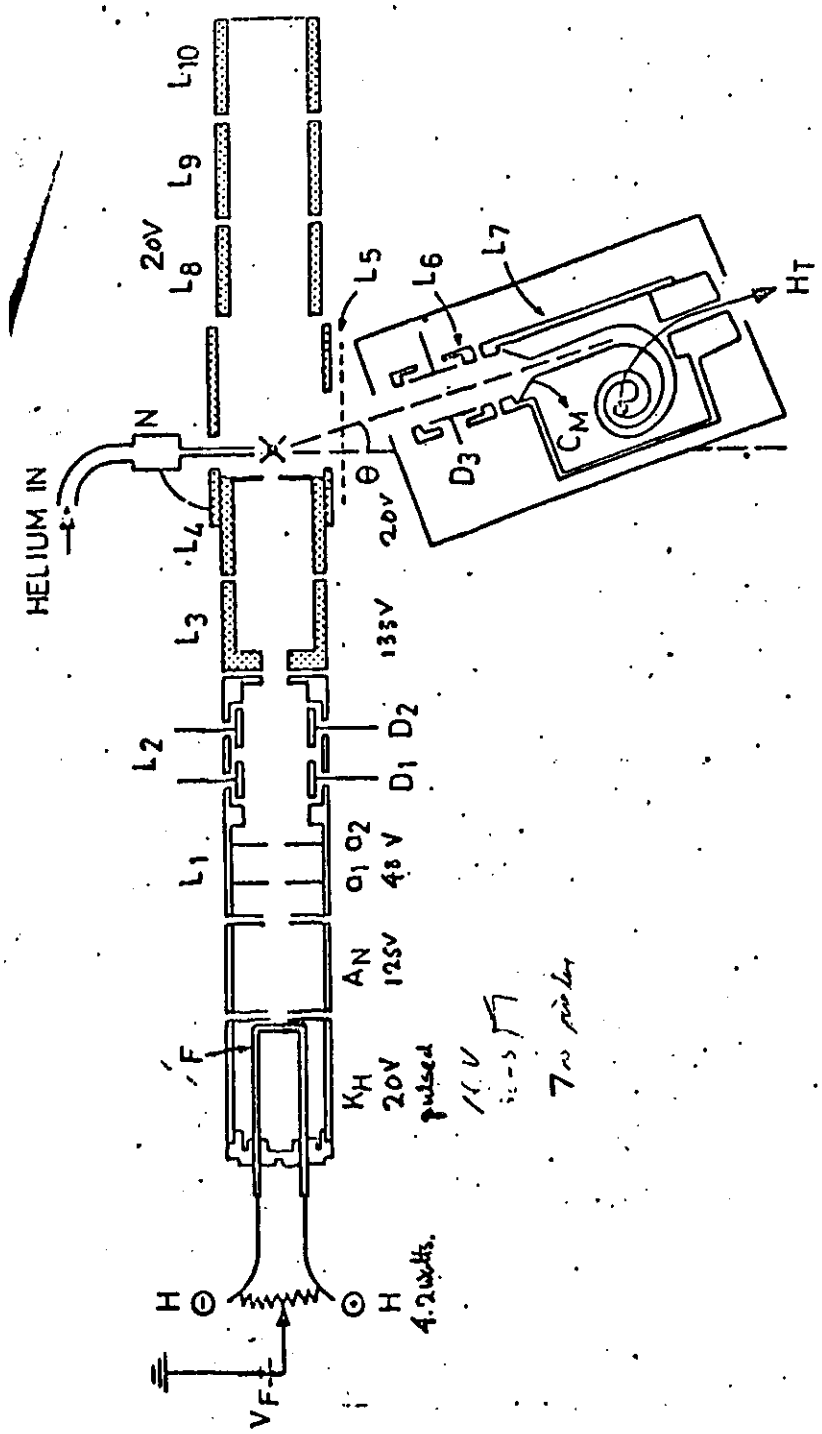


FIG 3: DETAILS OF THE EXPERIMENT ARRANGEMENT. THE LASER BEAM ENTRY IS PERPENDICULAR TO THE PAGE AT THE COLLISION REGION (MARKED X)

Low-energy electron beams are plagued by the built-up of charge on insulating deposits on the surfaces of electrodes and on insulators. Ours is no exception.

The Laser Beam

The layout of the optics is shown in Fig. 4. The "JK" Nd-YAG laser produces up to 200 multi Joules in a 17n Sec (FWHM) pulse at a repetition rate of 20pps. It is run multimode, in practice in a low order. The jitter of the output relative to the Pockels cell trigger is typically less than 5n sec and the output energy is stable for long periods. The beam is expanded and focussed through the interaction region.

The plane of the gas needle jet is imaged on a card at 6.5 times magnification where a clear image of the tip of the needle jet can be seen in He-Ne illumination. The experiment was setup with a small box (later removed) concentric with the aperture in L4 so that the position of the axis could be marked with a precision of 0.25mm. Fig. shows the laser beam profile for one and ten shots. The peak intensity is of the order of $2 \times 10^9$ W/cm$^2$. The signal strength is proportional to the total number of photons passing through the interaction volume defined by the intersection of the electron beam with the helium jet, during a run.

Synchronisation

The laser was synchronised to the electron beam by comparing the arrival time of pulses from scattered electrons with that of a pulse produced when the laser beam was steered to generate a weak plasma at the tip of the gas needle jet.

The Gas Needle Jet

This is a hypodermic needle supplied with research grade He gas at about 8 torr at room temperature. The supply line passes through a liquid nitrogen bath before reaching the flow control needle valve. Standard high purity He was found to give rise to substantial background at electron beam energies about 10 volts. With the jet off, the base pressure of the system $\lesssim 10^{-7}$ torr. The "pressure" in the jet at the interaction point is estimated to be $\sim 10^{-3}$ torr. With the jet on, the ambient pressure rises to $10^{-6}$ torr.

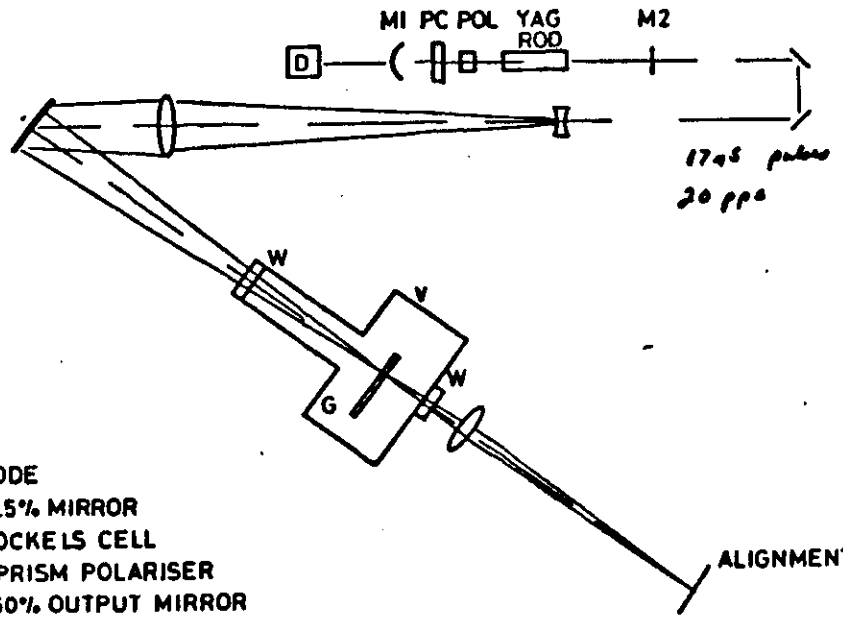


D: DIODE
MI: 99.5% MIRROR
PC: POCKELS CELL
POL: PRISM POLARISER
M2: 50% OUTPUT MIRROR
G: ELECTRON GUN
V: VACUUM VESSEL
W: INPUT AND OUTPUT WINDOWS

NOT TO SCALE

FIG. 4 LAYOUT OF OPTICS

The Detection System

The channeltron is mounted inside two separate, independently earthed, copper boxes with a small entrance aperture upstream of which is placed a copper cylinder equipped with deflection plates. Bias voltages applied to this cylinder and to the mouth of the channeltron prevent the detection of almost all electrons or ions. The anode of the channeltron is capacitatively coupled to an amplifier which feeds a gated discriminator. The channeltron is operated at a voltage somewhat below the saturated amplification level. In DC operation the maximum count rate of the channeltron is a few times $10^4$ per second. However, it will count several particles in a short burst at an instantaneous rate of almost $10^6$ per second. We adjust the count rate in the experiment (via the gas needle jet flow or the cathode temperature) so that the rate at the metastable peak is of the order of one per four pulses. In this condition as many as one scattered electron per ten or a hundred pulses may be detected at the time of the electron beam pulse, despite the bias. The function of the gate is to prevent these being recorded by the computer system, which can only log one event per pulse.

The output from the discriminator is used to stop a 1MHz clock in the CAMAC unit which is started at the time the fire command is issued Fig. 2. When a stop signal is received, the CAMAC unit generates an interrupt to the computer. The computer reads the time of flight for the event, a laser on or off flag and the number of pulses since the last event of that type, and histograms data (laser on/off flight times, laser on/off elapsed pulses). The discriminator also feeds a scaler. Since this can record more than one event per pulse, comparison of the scaler with the sum of on and off computer events enables us to decide whether any correction for dead-time effects should be made. No correction has been required for the present data. The generation of new trigger pulses is suspended until the transfer of information is complete. Normally there is no interruption to the (overall) 40 pps rate. However, if the computer is engaged on another task a pause of from a few seconds to two minutes is introduced. The laser and the electron beam are not triggered during the pause.



Scattering Geometry

The momentum transfer from the electron to a He atom at the peak of the observed velocity distribution deflects it through an angle of $17\frac{1}{2}^{\circ}$ on average, with a spread of $2.4^{\circ}$. Estimates of the spread due to the divergence of the gas were made for laser-assisted events and for directly-produced events. The longitudinal spread is somewhat smaller for laser-assisted events because of the small size of the laser beam.

Time of Flight Distribution of Metastables

The observed distribution is quite sensible apart from the pronounced narrow spikes seen in the typical examples of Fig. 5. It is conceivable that the first spike is due to the detection of UV photons produced by metastable de-exciting on impact with the surface of L4 at the edges of the exit hole. This is, however, unlikely since no such explanation can account for the subsequent structure which is so similar to the first spike that it is likely to have the same cause. Because of delays in triggering, the "laser on" time distribution has a different registered clock time from the "laser off" distribution, by 180 μsec, but it also shows the same spikes, so missing binary digits are not the cause. There is the possibility that we are in fact observing scattered electrons due to occasional after-pulsing of the electron gun. However, the rather large (in this context) width (~ 4 μsec) of the peaks makes this also unlikely.

Difference Measurements

When running at or close to the peak of the direct metastable production very high statistics were obtained. However, in order to demonstrate the existence of the laser-assisted process it was necessary to sit at the bottom of the steepest part of the direct process excitation curve, where small changes in electron-beam energy can give large variations in count rate. In one set of runs a signal was seen which disappeared when the laser beam was blocked and reappeared when it was unblocked. However, we now believe the timing was in error during these runs.

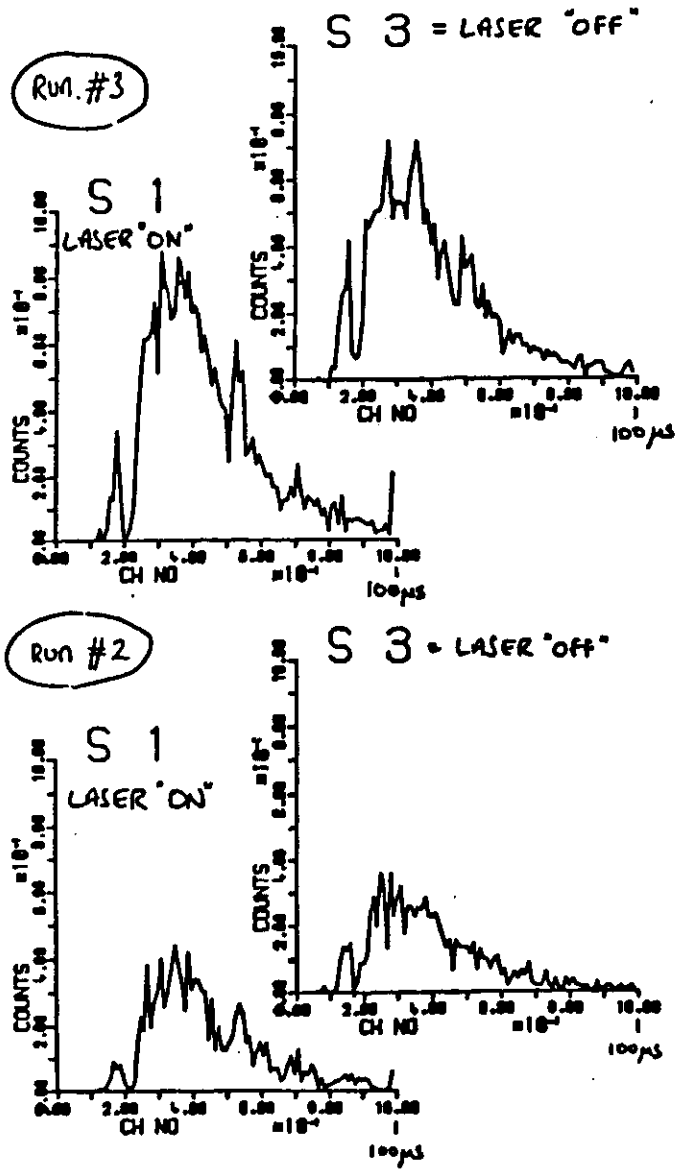


Fig Laser "on" and laser "off" time of flight spectra.



Subsequently, attempts were made with supposedly better timing but no reproducible signal was seen. A parasitic signal was however seen with deliberately bad timing. One possibility is that some of the apparent laser-assisted events are due to low concentrations of contaminants in the jet which vary from time to time.

A multiphoton process might then occasionally occur giving spurious events. However, the difference time spectrum ought to show a substantially different mean velocity in this case and it does not. Alternatively, an occasional laser pulse producing a small amount of surface ionisation on the electrodes defining the beam energy could cause a minute shift in beam voltage and thus an increase (or decrease) in direct process background, but only when sitting on the sloping part of the curve and thus not visible when simple null tests were made at the peak of the curve.